Proceedings of the NROCK 2023
The IV Nordic Symposium on
Rock Mechanics and Rock Engineering
ISBN 978-9935-9436-2-0
DOI 10.33112/nrock2023.12

Full-scale pullout tests of rock anchors in limestone testing rock mass uplift failure

Bjarte Grindheim (Bjarte.grindheim@ntnu.no)

B. Grindheim, C. C. Li
Department of Geoscience and Petroleum, Norwegian University of Science and Technology (NTNU), Trondheim, Norway
A. H. Høien
Norwegian Public Roads Administration (NPRA), Bergen, Norway

ABSTRACT

Rock anchors is a high-capacity reinforcement measure used to stabilise large-scale infrastructure. In principle, they can fail in four ways: (1) rock mass uplift failure; (2) grout-rock interface failure; (3) tendon-grout interface failure; and (4) steel tendon tensile failure. Full-scale field uplift tests were performed in a limestone quarry. The tests were designed to test failure mode 1, rock mass uplift failure, aiming to estimate the uplift load-bearing capacity of the rock mass. The tests achieved a higher rock mass capacity than what was calculated with the "weight over overlying rock cone" method and using presumptive shear strength values along the assumed failure cone. The failure shape showed to be structurally dependent on the rock mass structure, and a uniform cone was not developed. Stress measurements showed an increase in the horizontal stress in the rock mass during the pulling of the anchor, which indicates the formation of a load arch in the rock mass. The results showed that the current design method is over conservative in a medium strong rock mass and there is a need for development in the design method for strong and unweathered rock masses.

KEYWORDS

Rock Anchor; rock mass failure; load bearing arch; failure surface; field test

INTRODUCTION

Rock anchors are high-capacity reinforcement measures used to support and stabilise large scale infrastructures (Hanna, 1982), such as dams, abutments of bridges, road cuts, slopes (Xanthakos, 1991), wind turbines (Yan et al., 2013; Shabanimashcool et al., 2018), and submerged structures (Mothersille and Littlejohn, 2012; Roesen and Trankjær, 2021). The forces from the structures are transferred to the competent ground through the rock anchors. The rock anchors transfer load through tension, the tensional load in the anchor is resisted by the shear strength of the surrounding ground (Hanna, 1982). The correct usage and design of rock anchors requires knowledge and understanding of their failure modes (Tayeh et al., 2019). Rock anchors can in principle fail in four ways, which are (1) rock mass uplift failure; (2) grout-rock bond or interface failure; (3) tendon-grout or interface failure; and (4) steel tendon tensile failure (Littlejohn and Bruce, 1977; Brown, 2015). The failure modes are illustrated in Figure 1. The weakest of the four failure modes determines the capacity of the anchoring system (Pease and Kulhawy, 1984; Kim and Cho, 2012).

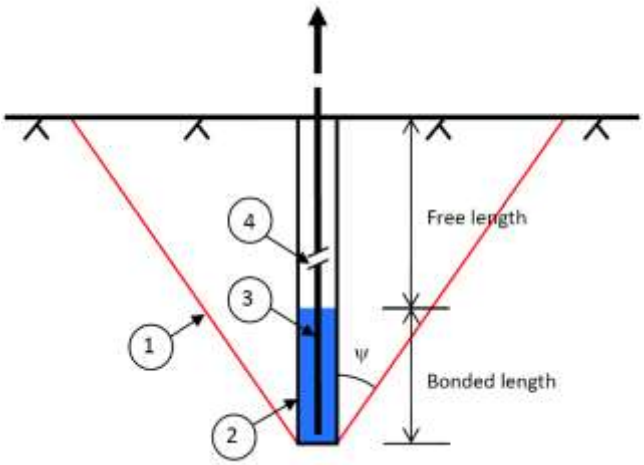

Figure 1. Four principal failure modes of a rock anchor from literature: (1) rock mass uplift failure; (2) grout-rock bond or interface failure; (3) tendon-grout bond or interface failure; and (4) steel tendon tensile failure.

The uplift capacity of the rock mass around a rock anchor is calculated based upon the dead weight of an inverted rock cone surrounding the anchor (Xanthakos, 1991) and/or the shear resistance of the rock mass along the cone with presumptive or back calculated shear strength values (Brown, 2015). The dead weight calculations alone are conservative as the shear and tensile strength of the rock mass is ignored (Xanthakos, 1991). Bruce (1976) showed that these estimations underestimated the rock mass capacity by one order of magnitude. There are very few documented cases of rock mass uplift failure (Xanthakos, 1991). The observed rock mass uplift failures in literature are from shallow anchoring depths (Brown, 2015), such as Bruce (1976), Ismael et al. (1979), Ismael (1982), Dados (1984), Weerasinghe and Littlejohn (1997), García-Wolfrum et al. (2007) and Thomas-Lepine (2012).

Brown (2015) listed several deficiencies with the current design method against failure mode 1. These deficiencies are mentioned in the following. The induced stresses in the overlying rock mass from the anchor is not considered. The effect of the anisotropy of the rock mass on the stresses and failure shape is not considered. The tests with rock mass uplift failure were done with shallow anchoring depths, which questions if this is representative for larger and longer anchors. The literature has shown how the rock mass structure affects the failure shape of shallow anchors, however for deeper anchors the rock mass structure might not be as controlling and the assumption of a 90^{o} uplift cone might not be valid. The usage of presumptive and back calculated shear and tensile strength values based on a “theoretical” failure cone to calculate the rock mass capacity is questionable, as the variability of the strength parameters within the varying local rock mass structure is not considered as well as the progressive and complex nature of the rock mass failure. Bruce (1976) also questioned if rock mass failure occurs for anchors installed deeper than 2 m, since he only observed rock mass uplift failure in anchors installed at depths less than 2 m and the other failure modes occurred in the anchors installed deeper than 2 m.

Testing of full-scale rock anchors in real rock masses are important due to the uncertainties and deficiencies of the current design methods. The design method against rock mass uplift failure is considered as the least satisfactory and therefore it was investigated through full-scale uplift tests in a limestone quarry. The tests were highly instrumented to measure the stresses and localise the fracture plane. The novelty of the tests was to increase the understanding of the uplift failure of the rock mass through a thorough instrumentation scheme, which may be used to develop a more precise dimensioning method against rock mass uplift failure.

1. TEST ARRANGEMENT AND PROCEDURE

1.1. Test setup

The full-scale field tests were planned to investigate the uplift capacity of the rock mass surrounding rock anchors. Four anchors were installed in the limestone quarry of Verdalskalk AS in Tromsdalen, Norway. The anchors were 64 mm bar anchors with lengths 2.5 m and 3 m, the steel had a Young's modulus of 200 GPa and nominal tensile strength of 1000 MPa. They were installed with endplates in 140 mm boreholes. The anchoring depths of the

anchors were 1 m and 1.5 m. On top of the anchors were a steel beam placed, the beam had a span of 3 m, which was decided based upon the anchoring depths and an apex angle of 90° from literature (Littlejohn and Bruce, 1977; Brown, 2015). A hydraulic jack was placed on top of the beam at the centre around the anchor before the test.

The test site was in a corner of an open pit quarry with a relatively flat surface and strong unweathered limestone. The rock mass was homogeneous with a uniaxial compressive strength (UCS) of 115 MPa, ranging from 106.7 to 121.4 MPa. Three joint sets were found and measured in the rock mass. All the joints were planar and rough. Close to the bench crest, there were signs of blast damage in the rock mass. Therefore, the holes were drilled with a minimum distance of 3 m to bench crest and a minimum spacing of 3 m in between the anchors. Around the two longest anchors, there were drilled holes with 102 mm diameter to a depth of 2.5 m for the instrumentation. All drilling was done pneumatically.

Concrete platforms had to be casted for the beam to be levelled on the surface. The formwork of the platforms was levelled by a leveller and then filled with rocks and grout. The grout was left to harden for four weeks until the tests. The anchors were lifted into the boreholes by an excavator and then grouted from the bottom and up with a water-cement ratio (W/C) of 0.42 with an average strength of 56.2 MPa after 28-days.

The instrumentation of the anchors varied in the tests. On all the anchors, the oil pressure was measured to calculate the anchor load and the vertical displacement of the anchor was measured by a thread extensometer (LVDT). The surface heaving of the rock mass was measured by six LVDTs fastened on an aluminium beam, which was placed under the steel beam, with the threads fastened to small bolts on the rock surface. The two longest anchors installed at 1.5 m depth, anchors A1.5m and B1.5m, were highly instrumented. There were installed load cells and extensometers in the rock mass around these anchors. Two observation holes at each anchor were drilled to map the jointing in the rock mass before and after the tests with acoustic and optic televiewer. Geophones were used to monitor the seismic signals from the rock mass when it fractured during the tests of the three anchors B1m, A1.5m and B1.5m. The P-wave velocity of the rock mass was estimated to be 2000 m/s.

1.2. Test procedure

The test arrangement of anchor A1.5m is shown in Figure 2. The beam was placed on two concrete platforms with the anchor in centre. A 3500-kN hydraulic jack was placed on top of the anchor and beam, the area in centre of the beam was fortified with a 5 cm thick steel plate. The hydraulic jack was pressurised from a gasoline driven hydraulic pump and a booster unit with capacity of 700 bar.

Figure 2. Test arrangement of anchor A1.5m. The steel beam is placed upon two concrete platforms with a hydraulic jack on top on the anchor. The LVDTs on the aluminium beam measured the surface heaving of the rock mass and the yellow geophones measured the microseismic activity during the test.

The load was applied on the anchors in two ways. The two shortest anchors, A1m and B1m, were loaded first in a continuous manner with a load rate from 5-7.5 kN/s until failure occurred. After failure, the displacement of the anchor was continued until the end of the jack stroke, and then the jack was repositioned, and the displacement was continued until the anchor load was low enough to be lifted by an excavator. The two longest anchors, A1.5m and B1.5m, were loaded stepwise and each load step was held for 5 minutes due to the borehole extensometer were only logged once every 5 minutes. The load steps had an average load rate of around 11.5 kN/s. The load in the system dropped if the pump was stopped, therefore the operator had to keep a little flow going to maintain the load at the desired level. All the pullout tests were performed in the period 15th and 16th June 2022.

After the tests were finished, the rock anchors were removed and the loose rocks around the location of the anchors were removed by an excavator. The failure surfaces were then cleaned and scanned with the lidar on an iPad.

2. RESULTS AND ANALYSIS

The test results are summarised in Table 1 for all the tests. The results from the test of anchor B1.5m is shown more in detail, but the results from the other tests were similar. The load and displacement curve of the anchor is shown in Figure 3. The load increased linearly in the beginning (i.e., elastic stage), then it started to bend (i.e., plastic stage) before reaching the peak load. After peak load, the load dropped gradually, the drops at 210 mm and 420 mm marks the end of the jack stroke. The rock mass surface heaving around anchor B1.5m is shown in Figure 4. The surface heaving of all the anchors was approximately 10% of the anchor displacement closest to the anchor until 200 mm displacement, then it increased to 15-20% of the anchor displacement for the remaining of the tests. The heaving decreased with distance from the anchor.

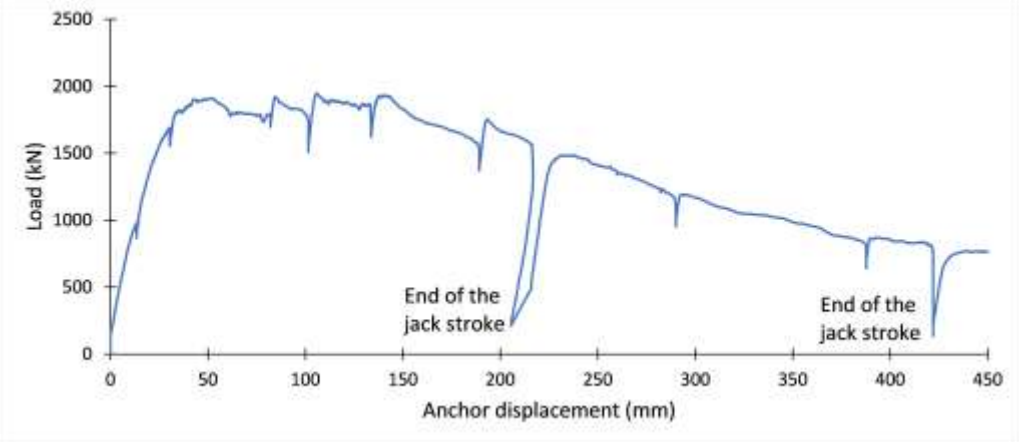

Figure 3. Load-vertical displacement curve of anchor B1.5m. The load drops at 210 mm and 420 mm displacement marks the end of the jack stroke.

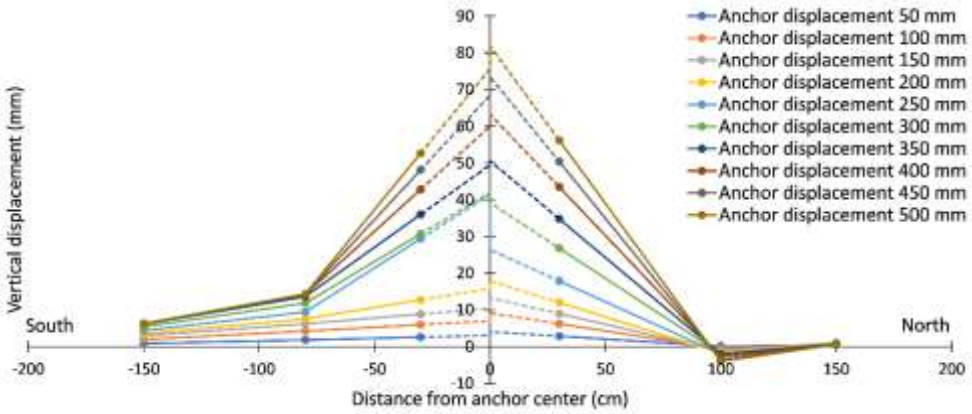

Figure 4. Rock mass surface heaving around anchor B1.5m at distance, where the dotted lines are extrapolations.

The horizontal stress and vertical displacement of the rock mass was measured around anchors A1.5m and B1.5m with load cells and borehole extensometers. These measurements for anchor B1.5m are presented in Figure 5. The horizontal stress in the rock mass increased in the elastic loading of the anchor and it became more unstable in the plastic and post peak stage of the loading, as seen in Figure 5(a) and Figure 5(b). The vertical displacement in the rock mass increased most in between 55-95 cm depth at 44 cm from the anchor (Figure 5(c)) and 45-85 cm at 103 cm from the anchor (Figure 5(d)).

The lidar scan of the failure surface combined with the location of the seismic events and profiles along the failure surface are shown in Figure 6. The seismic events are plotted in the north-east plane with all events on the surface, as depth measurements were unreliable since all the geophones were placed on the surface. The profile in the east-west direction was longer as two of the joint sets in the rock mass formed a wedge in that direction, the failure surfaces of all the tests had this asymmetrical shape with a wedge formed in that direction. The average apex angle was measured from the profiles (Figure 6(b)), for anchor B1.5m the apex angle was 132°. The results from all tests are summarised in Table 1.

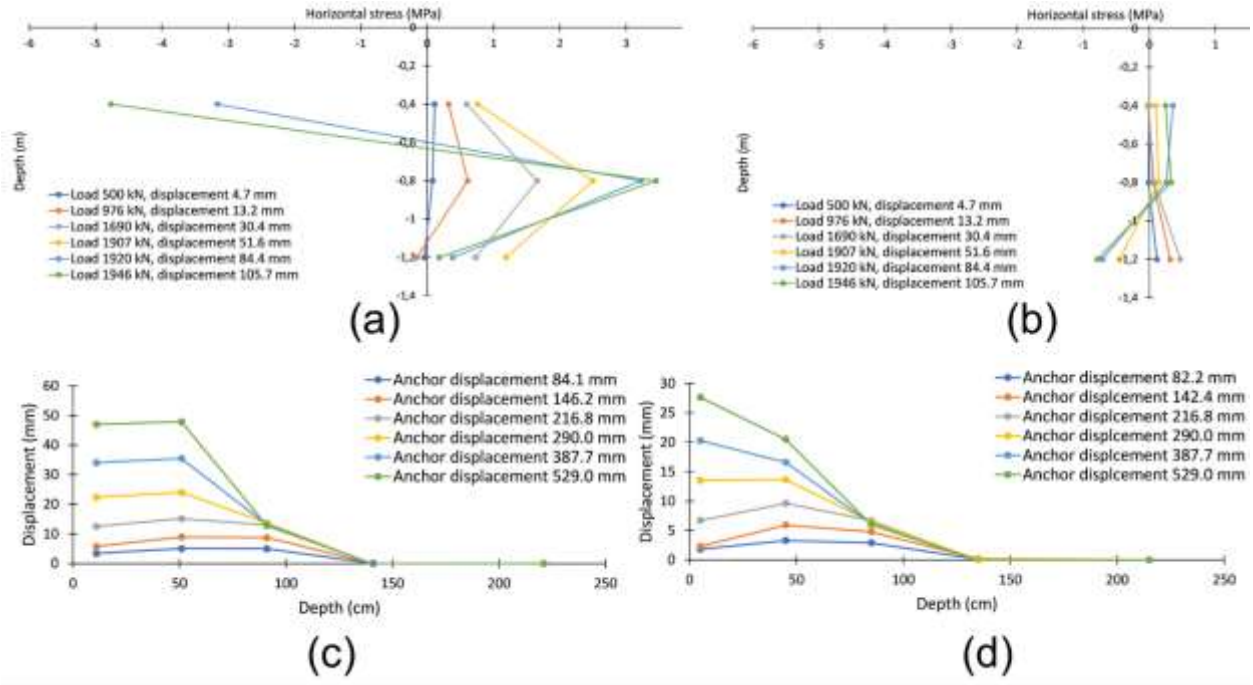

Figure 5. Horizontal stress measurements and borehole extensometer measurements around anchor B1.5m. (a) horizontal stress 41 cm west of the anchor; (b) horizontal stress 49 cm east of the anchor; (c) borehole extensometer measurements 44 cm southwest of the anchor; and (d) borehole extensometer measurement 103 cm southwest of anchor.

Table 1. Summary of test results from all tests.

Anchor no.	**A1m**	**B1m**	**A1.5m**	**B1.5m**
Bonded section (m)	0.9	0.9	1.4	1.4
Maximum uplift load (kN)	2461.6	2309.5	2422.6	1946.2
Anchor displacement at max load (mm)	66.7	59.6	71.8	105.7
Cone volume (m^3)	2.28	2.27	3.55	3.66
Apex angle (degrees)				
- *from extensometers*	-	-	105-170	105-170
- *from televiewer*	-	-	-	125
- *from profiles*	127	131	142	132

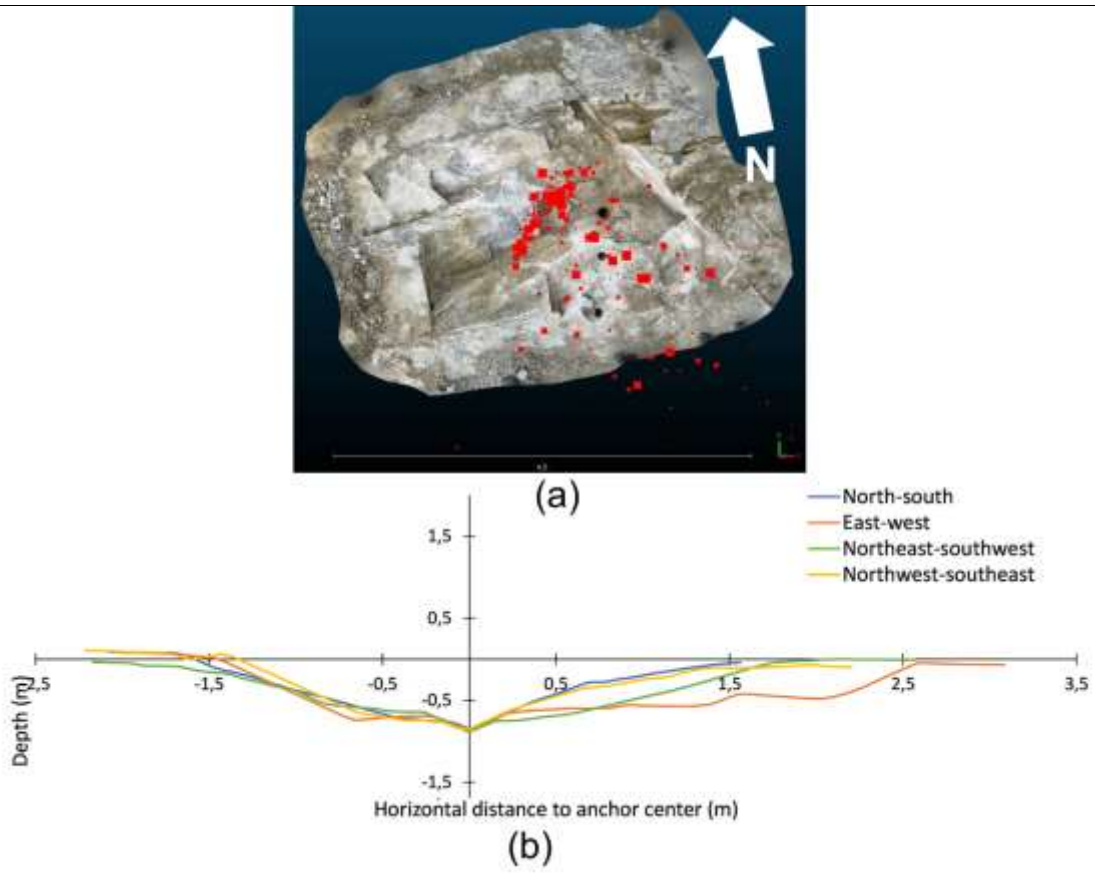

Figure 6. Lidar and seismic data: (a) Lidar scan of failure surface around anchor B1.5m with the location of the seismic events; (b) profiles of the failure surface. The relative size of the seismic events is shown by the size of the dots.

3. DISCUSSION

3.1. Failure shape and failure mode

In literature, the width and location of the apex angle varies, the location of the apex angle has been placed at the bottom or at the middle of the bonded section (Littlejohn and Bruce, 1977; Brown, 2015). These tests were designed with the assumption of a 90º apex angle placed at the bottom of the bonded section. Wyllie (1999) discussed the effect of joints on the shape of the failure cone, horizontal jointing would result in a wider apex angle while vertical jointing would result in a smaller apex angle. The measured apex angles in the four tests were ranging from 127-142º, which is greater than what is mentioned in most literature and standards. The commonly recommended apex angles to use are in between 60-90º, with 60º for weak rock masses and 90º for stronger rock masses. García-Wolfrum et al. (2007) showed on small intact rock samples that the apex angle is not constant, but smallest at the bottom and increasing towards the surface. The location of the apex angle in these tests varied in depth from 0.59-0.83 m below the surface, where non of them occurred at the bottom of the bonded section.

The failure mode seen in these tests was a combination of rock mass failure and bond failure between grout-rock. The deepest parts of the bonded length had interfacial bond failure between grout-rock. This was observed when the failure surface was cleaned, then the lowest part of the borehole was still intact in the rock mass as shown in Figure 7. Weerasinghe and Littlejohn (1997) also observed combination of rock mass failure and bond failure in weak mudstone. They suggested that the apex lies within the top 0.5 m of the fixed anchor, and that bond failure occurs below 0.5 m depth, which is a possible explanation for the observed failure in these tests since the depth of the failure was consistent between 0.59-0.83 m even though the bonded lengths varied between 0.9-1.4 m depth. Another explanation is due to the measured apex angles, since the angles were wider than what is shown in literature, then the area affected by the tests were wider than the length of the beam. This resulted in the beam

confining the outer area of the affected rock mass, which increased the rock mass strength. Therefore, a combined failure occurred, with failure at the rock-grout interface in the lower part of the bonded section and in the rock mass in the upper part, as illustrated in Figure 8.

Figure 7. Intact borehole at the bottom of the failure crater after anchor B1.5m.

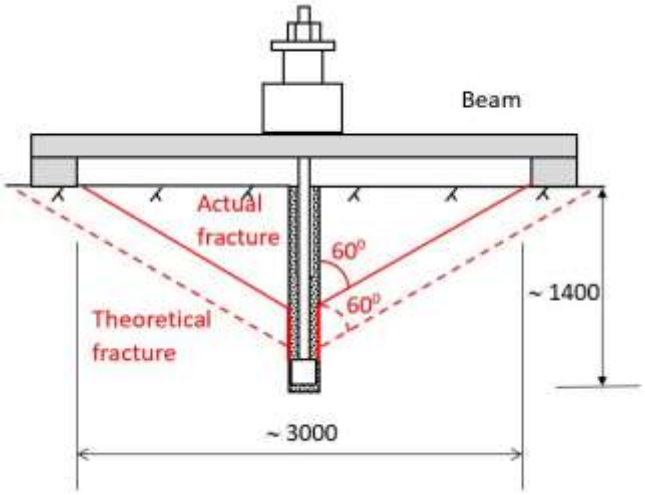

Figure 8. Possible failure shape of the anchors tested.

The failure mode of the rock mass is complex. The failure shape is also affected by the pre-existing joints in the rock mass. During the tests, it was obvious that the pre-existing joints opened first, as shown in Figure 9. From the seismic measurements in Figure 6, the most part of the failure crater has been developed along the pre-existing joints. There are no or only very small events in the west, northwest, and north side of the crater, which indicate that the intact rock has not fractured in these parts. The colour of the failure surface of these parts are also slightly miscoloured which indicate weathering, which means that these are pre-existing joints in the rock mass.

Figure 9. Surface cracking around anchor B1.5m after the test finished.

3.2. Load capacity of the rock mass

The anchor capacity of the tests was calculated based upon the design methods given by the Norwegian Public Roads Administration (NPRA, 2018) and from back calculation of historical data. The design methods given by NPRA, which uses the dead weight of the overlying rock and presumptive shear strength of the rock mass, resulted in very conservative design. The recommended cohesion for a rock mass with three joint sets and less than 20 joints per square meter was 50 kPa. The historical data came from tests in intact rock (García-Wolfrum et al., 2007), carboniferous strata (Bruce, 1976), a very weak shale (Littlejohn and Bruce, 1977), and granitic mass (Dados, 1984). The rock mass strength used in the calculation was based upon an average from the historical data rounded down to the closest half MPa. The rounding down of the rock mass strength was done due to lack of data and the scale difference between the tests of García-Wolfrum et al. (2007) and the test performed here. The estimated uplift capacity, sum of weight and max shear resistance, from NPRA (2018) was 166 kN and 403 kN for 0.9 m and 1.4 m depth, respectively, while the capacity was 1049 kN and 2388 kN from the back calculation with historical data. The uplift capacity estimations are summarised in Table 2.

Table 2. Anchor uplift capacity estimation based upon presumptive values from (NPRA, 2018) and back calculation from historical data.

Depth (m)	Apex angle (degrees)	Cohesion from back calculation (MPa)	Presumptive cohesion from NPRA (2018) (kPa)	Weight force (kN)	Max shear resistance from back calculation (kN)	Max shear resistance from NPRA (2018) design (kN)
0.9	90	0.5	50	20.2	1029	146
1.4	90	0.5	50	76.1	2312	327

The measured uplift capacity was much higher than the estimate with the recommended method from NPRA (2018). Therefore, it is important to understand the difference between the measured uplift capacity compared to the estimated uplift capacity with the current design methods from a rock mechanics perspective. The current design method is very simplified and conservative. The rock mass characteristics are not used in the design, the design method only uses the density of the rock to calculate the weight of overlying rock, and the number of joint sets to estimate the shear strength of the rock mass through a table of presumptive values given by NPRA (2018). The estimated capacity based upon historical data was closer to the achieved capacities, but they underestimated the capacity of the anchors with short, bonded section and slightly overestimated the capacity of the anchors with a longer bonded section. The back calculated cohesion from García-Wolfrum et al. (2007), Dados (1984), Littlejohn and Bruce (1977) and Bruce (1976) showed large variations depending on the rock types and rock masses. There are many assumptions involved with the back calculations, it was assumed that the failure surface was an inverted cone, that the cohesion was uniform in the rock mass, and an apex angle of 90^{o} when nothing else has been stated. All calculations have been done from the bottom of the embedment depth. The back calculations indicated that the cohesion is greatly influenced by the rock type and joint density in the rock mass. Unfortunately, there are very few full-scale tests that reports of rock mass failure in anchor uplift tests, this was also seen and reported by Xanthakos (1991) which wrote "there is an impressive scarcity of data on anchor failure in rock mass, hence documentation of stability theories is not readily available". Due to this lack of data, the design methods against rock mass failure have been on the conservative side.

In Norway, the rock masses are mostly strong and unweathered. These rock masses have high load carrying capacities, which will result in underestimations of the load capacity with the current dimensioning method, as has been shown in these tests in a medium strong rock mass. Bruce (1976) concluded with that the uplift capacity was very sensitive to the degree of weathering, and much less sensitive to the rock mass structure. Since the design method is supposed to work for all rock masses, it is made to work in weathered rock masses which is why it is so conservative in unweathered rock masses. Therefore, there is a need to update or make a new design method for areas which have strong and unweathered rock masses. This could reduce the size of the anchors, which would be more environmentally friendly and more cost effective.

3.3. Stress distribution in the rock mass

The induced stresses in the rock mass have been questioned by Brown (2015). These tests show a slight increase in the horizontal stress around the anchor during the uplift tests before the peak load has been reached. The increase in horizontal stress is an indication that a load arch is formed in the rock mass during the pulling of the anchor. This has formerly only been shown in small scale laboratory tests with concrete blocks by Grindheim et al. (2022). The load arching in the rock mass contribute to increased rock mass capacity and therefore also making the current design method against rock mass uplift even more conservative.

4. CONCLUSIONS

Rock mass uplift tests has been performed in a limestone rock mass to investigate the rock mass uplift capacity and failure process. The rock mass capacity was much higher than what was calculated with presumptive values found in the recommended guideline in Norway. The estimations based upon back calculations from historical data was more accurate. The apex angle measured, 120-140^{o}, was higher than the recommendation in literature, 60-90^{o}. The horizontal stress in the rock mass increased during the tests, which indicates the formation of a load arch around the anchor as described in Grindheim et al. (2022).

These field tests shows that the current design method for rock mass uplift failure is very conservative and inaccurate for a medium strong rock mass. This has also been shown in literature earlier, but the method has not been updated due to very few documented cases of rock mass failure. In areas with medium strong or stronger rock masses, the rock mass capacity is much higher than the current design and results in over dimensioned anchors.

5. FURTHER RESEARCH

These field tests demonstrated how the rock mass fails around shallow anchors installed in a medium strong rock mass. The endplates of the anchors combined with the steel beam resulted in rock mass failure. The rock mass heaved close to the anchor with a distance less than 150 cm and the fracturing was greatest above the endplate at a depth of 60-80 cm at distances 40 cm to 100 cm from the anchor. The pre-existing joints in the rock mass affected the failure shape. In future research, it would be necessary to test anchors at increasing depths to see if or how the failure shape and mechanism changes with depth. Brown (2015) argued for that the joints in the rock mass would have less effect on the failure shape and mechanism at large depths. One could also argue that the rock mass is much stronger than the grout and steel so at a certain depth the grout or steel would always be the weakest part of the anchoring system, testing to find this depth level would be very useful for anchor design. Bruce (1976) saw that the rock mass in most cases was the strongest part of the anchoring system when installed at greater depths (>2 m).

6. ACKNOWLEDGEMENTS

The authors acknowledge the financial support of the Research Council of Norway through the research project ROCARC, project number 303448. The partners of the project are NTNU, SINTEF, NGI, The Arctic University of Norway (UiT), Norwegian Association of Rock Mechanics (NBG), Norwegian Public Roads Administration (NPRA), Multiconsult AS, Norconsult AS and NORSAR. The authors thank Simon Alexander Hagen in SINTEF and Jon Runar Drotninghaug for their enthusiastic participation in the field tests and Noralf Vedvik for his technical assistance in manufacturing. The authors are also grateful to Verdalkalk AS, especially Ørjan Sjöström, for the use of their quarry and all their help.

REFERENCES

Brown, E.T., 2015. Rock engineering design of post-tensioned anchors for dams - a review. Journal of Rock Mechanics and Geotechnical Engineering 7, 1–13. DOI: doi.org/10.1016/j.jrmge.2014.08.001.

Bruce, D.A., 1976. The Design and Performance of Prestressed Rock Anchors with Particular Reference to Load Transfer Mechanisms (As reproduced by ProQuest LLC 2014 (UMI U433767)). Ph.D. thesis. University of Aberdeen. Aberdeen, Scotland.

Dados, A.T., 1984. Design of anchors in horizontally jointed rocks. Journal of Geotechnical Engineering 110, 1637–1647. DOI: doi.org/10.1061/(ASCE)0733-9410(1984)110:11(1637).

Grindheim, B., Aasbø, K.S., Høien, A.H., Li, C.C., 2022. Small block model tests for the behaviour of a blocky rock mass under a concentrated rock anchor load. Geotechnical and Geological Engineering 40, 5813-5830. DOI: doi.org/10.1007/s10706-022-02251-1.

García-Wolfrum, S., Serrano, A., Olalla, C., 2007. Model failure tests on rock anchors, in: 11th Congress of the International Society for Rock Mechanics: The Second Half Century of Rock Mechanics, Taylor & Francis Group, Lisbon, Portugal. pp. 339–342.

Hanna, T.H., 1982. Foundations in Tension: Ground Anchors. Trans Tech Publications and McGraw-Hill Book Company, Clausthal, Germany.

Ismael, N.F., 1982. Design of shallow rock-anchored foundations. Canadian Geotechnical Journal 19, 463-471. DOI: doi.org/10.1139/t82-050.

Ismael, N.F., Radhakrishna, H.S., Klym, T.W., 1979. Uplift capacity of rock anchor groups. IEEE Transactions on Power Apparatus and Systems 98, 1653–1658. DOI: doi.org/10.1109/TPAS.1979.319483.

Kim, H.K., Cho, N.J., 2012. A design method to incur ductile failure of rock anchors subjected to tensile loads. Electronic Journal of Geotechnical Engineering 17, 2737–2746.

Littlejohn, G.S., Bruce, D.A., 1977. Rock anchors - state of the art. Foundation publications LTD., Brentwood, Essex, England.

Mothersille, D., Littlejohn, S., 2012. Grouting of anchors to resist hydrostatic uplift at Burnley tunnel, Melbourne, Australia, in: Proceedings of the Fourth International Conference on Grouting and Deep Mixing, American Society of Civil Engineers, New Orleans, Louisiana, USA. pp. 1073– 1084.

NPRA, 2018. Handbook V220 - Geotechnics in Road Construction (in Norwegian). Norwegian Public Roads Administration (Statens vegvesen), Oslo, Norway.

Pease, K.A., Kulhawy, F.H., 1984. Load Transfer Mechanisms in Rock Sockets and Anchors. Project 1493-1 EPRI EL-3777. Electric Power Research Institute. Ithaca, New York, USA.

Roesen, B.S., Trankjær, H., 2021. Permanent uplift anchors in Copenhagen limestone, in: IOP Conference Series: Earth and Environmental Science 710, IOP Publishing, Helsinki, Finland. p. 10.

Shabanimashcool, M., Olsson, R., Valstad, T., Lande, E.J., Berzins, A., Tuominen, K., Lapsins, J., 2018. Numerical modelling of anchored foundation for wind turbine generators, wtg (in Norwegian), in: Fjellsprengningsdagen - Bergmekanikkdagen - Geoteknikkdagen, NFF, NBG, NGF, Oslo, Norway. pp. 18.1–18.24.

Tayeh, B.A., El dada, Z.M., Shihada, S., Yusuf, M.O., 2019. Pull-out behavior of post installed rebar connections using chemical adhesives and cement based binders. Jorunal of King Saud University - Engineering Sciences 31, 332–339. DOI: doi.org/10.1016/j.jksues.2017.11.005.

Thomas-Lepine, C., 2012. Rock bolts - Improved design and possibilities. Master's thesis. Norwegian University of Science and Technology (NTNU). Trondheim, Norway.

Weerasinghe, R.B., Littlejohn, G.S., 1997. Uplift capacity of shallow anchorages in weak mudstone, in: Ground Anchorages and Anchored Structures: Proceedings of the International Conference, Thomas Telford Publishing, London, England. pp. 23–33.

Wyllie, D.C., 1999. Tension foundations. E & FN SPON, London and New York, England and USA. capter 9. pp. 310–359.

Xanthakos, P.P., 1991. Ground Anchors and Anchored Structures. Wiley Interscience, John Wiley & Sons, Inc., New York, USA.

Yan, S., Song, B.C., Sun, W., Yan, H., Yu, Q.L., 2013. Stress state analysis on a rock anchor rc foundation of wind driven generator, in: The 2013 World Congress on Advances on Structural Engineering and Mechanics, Daejeon Techno-Press, Jeju, Korea. pp. 2202–2213.